Climate Dynamics
https://doi.org/10.1007/s00382-024-07129-x

ORIGINAL ARTICLE

Daily temperature variation in March in East Asia from 1979 to 2020

So-Hee Kim[1] · Joong-Bae Ahn[1,2]

Received: 19 August 2023 / Accepted: 22 January 2024

Abstract
Recent change in the daily temperature variation (DTV) for March in East Asia is investigated. For this purpose, the effects of atmospheric circulation and global warming on the DTV in the region are analyzed using Japanese 55-year reanalysis data. Among the high-frequency variations in surface air temperature (SAT) during spring, the DTV in March showed a significant, increasing trend in East Asia during the four decades from 1979 to 2020. Composite analysis shows that the above-normal March DTV is associated with the anomalous anticyclonic circulation in the North Pacific and the anomalous cyclonic circulation over Russia. These atmospheric circulation anomalies lead to a greater meridional SAT gradient and tend to cause more mid-latitude pressure systems to pass over East Asia. Ultimately, the SAT in March becomes more variable due to enhanced thermal advection over East Asia. In addition, this pattern of circulation anomalies associated with a large March DTV includes features of a weak East Asian winter monsoon (EAWM) system. Meanwhile, regression analysis results using the EAWM and long-term global warming trend indices suggest that both the large-scale atmospheric circulation and global warming contribute significantly to the March DTV change in East Asia. In particular, heterogeneous warming rates and localized soil drying in East Asia during the study period likely explain the role of global warming on East Asian DTV in March.

Keywords Daily temperature · Temperature variations · East Asian winter monsoon · Global warming

1 Introduction

Climate change associated with global warming is recognized as a critical global issue of the 21st century due to its strong effects on the Earth's systems (IPCC 2014). In order to realistically assess and predict the impacts of climate change on natural and social systems, it is necessary to understand changes in climate variation, not just mean climate (Bathiany et al. 2018). That is because the frequency of extreme climate events can be statistically more sensitive to changes in the variance of the climate than to changes in the mean (Katz and Brown 1992; Wettstein and Mearns 2002; Schär et al. 2004). Various previous studies have revealed that high-frequency (day-to-day) variations in surface air temperature (SAT) can negatively affect both ecosystems and human health with respect to the adaptive capacity of organisms (Wolf et al. 2009; Zanobetti et al. 2012; Shi et al. 2015; Vicedo-Cabrera et al. 2016). Moreover, a change in high-frequency variations compared to low-frequency variations provides an opportunity for individuals to experience climate change. For example, more people were exposed to summer heatwaves in the 2010s than in the 1940s because more regions experienced three or more consecutive hot days (Vanos et al. 2015). Furthermore, Kotz et al. (2021) reported that an increase in high-frequency SAT variations negatively affects regional growth rates, reducing economic growth by around 5% on average, with stronger impacts in low-latitude and low-income regions (about a 12% reduction). Therefore, it is important to study the changes in high-frequency SAT variation, which is closely related to human life in many aspects.

Recent studies have suggested that Arctic amplification due to global warming decreases the meridional temperature gradient in the mid-latitudes of the Northern Hemisphere, and the resulting weakness in thermal advection contributes

✉ Joong-Bae Ahn
jbahn@pusan.ac.kr

[1] Department of Atmospheric Sciences, Pusan National University, 2, Busandaehak-ro 63beon-gil, Geumjeong-gu, Busan, South Korea

[2] Research Institute for Basic Sciences, Pusan National University, Busan, South Korea

Published online: 30 January 2024

to reduced SAT variation (Francis and Vavrus 2012; Screen 2014; Schneider et al. 2015). In this regard, various observational and model data show a decrease in high-frequency SAT variation at mid- and high latitudes in the Northern Hemisphere (Michaels et al. 1998; Screen 2014; Schneider et al. 2015; Wu et al. 2017). Simultaneously, increases in SAT variation have been reported in specific seasons or regions. Moberg et al. (2000) demonstrated that, based on eight observations in Europe, intra-monthly (30-day) SAT variation decreased by 5–10% in northeast Europe but increased by 5% in southwest Europe from 1880 to 1998. Schneider et al. (2015) showed that, as climate change progressed, SAT variation on the synoptic timescale (3–7 days) has mostly decreased in the mid-latitudes during summer and winter. However, they also observed an increase in SAT variation in some extratropical regions, particularly the Southern Ocean and central and eastern Europe in summer. Furthermore, Babina and Semenov (2019) found that SAT variations on a timescale of 8–20 days during the winter increased over southern Siberia in 2000–2015, compared to 1970–1999. In other words, the changes in SAT variation in recent decades exhibited spatial and temporal heterogeneity, emphasizing the need for more regional studies.

Meanwhile, many of the previous studies on SAT variations have focused on seasons with extreme temperature events, but SAT variations from an agricultural perspective, particularly in the spring, are also worth noting. In terms of dormancy periods and ontogenesis, the temperature in the early spring plays an important role in plant development (Chmielewski et al. 2004). Moreover, spring frost damage, which occurs when temperatures drop below freezing after sufficient heat has accumulated for seed germination, can be a major threat to overall agricultural production (Rigby and Porporato 2008). This may become more severe as global warming causes crops to bud or flower earlier than usual (Chmielewski et al. 2004). For example, in the spring of 2017, Switzerland and Germany experienced unprecedented frost damage as a cold Arctic air mass penetrated central and western Europe following an unusually warm period (Vitasse and Rebetez 2018). Meanwhile, Zohner et al. (2020) showed that the risk of late spring frost damage from 1959 to 2017 increased in Europe and East Asia more than in North America in response to climate change. Therefore, this study focuses on investigating changes in spring SAT variations, which have a devastating impact on agriculture in East Asia.

Regionally, SAT variation is often dominated by specific large-scale atmospheric circulation patterns (Dione et al. 2017). For example, based on observations in China from 1962 to 2008, Wu et al. (2017) found that the variation of summertime maximum temperatures correlated positively with the intensity of the Western Pacific subtropical high and the upper-level East Asian subtropical jet stream in the mid-lower Yangtze River basin. From this perspective, long-term changes in specific atmospheric circulations can often contribute to changes in SAT variation. Gong and Ho (2004) observed a significant decrease in wintertime SAT variations (November to March; 150 days) based on data from 155 stations in China and Korea from 1954 to 2001. They revealed that the positive phase of the Arctic Oscillation (AO) has a negative effect on SAT variations, and they concluded that the strengthening trend of the AO during the study period significantly explained the decreasing trend in SAT variations in the region. Thus, a study of atmospheric circulation associated with regional SAT variations can provide essential information for understanding changes in SAT variations in the region. Additionally, global warming may also directly affect SAT variations, so in this study, both atmospheric circulation and global warming are considered and investigated as possible causes of changes in SAT variations.

The purpose of this study is to examine and understand the changes in spring SAT variations over East Asia from 1979 to 2020. The data and methods used in the research are described in Sect. 2, and the climatology and long-term trends of spring SAT variations are examined in Sect. 3. All subsequent analyses focus on the SAT variations for March where significant changes were observed. Section 4 analyses the atmospheric circulation and climatic conditions that influence SAT variations. Then, in Sect. 5, the contribution of both atmospheric circulation and global warming to changes in SAT variations is statistically estimated, and the role of global warming is discussed in Sect. 6. Finally, a summary and conclusions from this study are presented in Sect. 7.

2 Data and methods

2.1 Data

We define the standard deviation of SAT over a period of time (e.g., season or month) as the daily temperature variation (DTV), which represents the SAT variation for that period (Michaels et al. 1998; Moberg et al. 2000; Schneider et al. 2015; Babina and Semenov 2019). Here, standard deviation is an appropriate measure to assess SAT variation from among various statistical measures (Moberg et al. 2000). The present study was conducted using Japanese 55-year reanalysis (JRA-55) data with a horizontal resolution of 1.25° × 1.25°, provided by the Japan Meteorological Agency (JMA 2013a, b). This dataset, which is an improvement on Japanese 25-year reanalysis (JRA-25), is considered to have a reduced systemic bias from the observations

(Ebita et al. 2011), and it has been frequently used in recent East Asian climate studies like Gong et al. (2021) and Nan et al. (2022). Monthly averaged variables used in this study include sea-level pressure (SLP), SAT, soil moisture, precipitation, geopotential height (GPH) at 850 hPa, 500 hPa and 300 hPa, and horizontal wind at 850 hPa and 300 hPa. Additionally, six-hour data on the SAT, GPH at 500 hPa, relative vorticity at 850 hPa, and temperature and horizontal wind at 1000 hPa are used. Among these variables, the SAT data are reprocessed into daily mean data to estimate DTV because the dataset does not provide data on a daily timescale. The analysis period for this study spans the spring season (March to May) over the 42 years from 1979 to 2020, but we examine the climatology and trends in DTV of the other seasons for reference (Figs. S1-S3). Thus, six-hour SAT is the only variable that covers not only spring but the other seasons as well.

In addition, daily mean temperature data from the Berkeley Earth Surface Temperatures (BEST) dataset (Rohde et al. 2013) was utilized to verify the long-term trends in DTV found in the reanalysis data. The BEST dataset contains approximately 39,000 observational records from 1880 to the present, and it is available at a $1^\circ \times 1^\circ$ horizontal resolution through the Berkeley Earth webpage (https://berkeleyearth.org/data/).

2.2 Extratropical cyclones and anticyclones

Mid-latitude synoptic-scale pressure systems are key drivers of daily weather changes (Okajima et al. 2021; Priestley and Catto 2022). They can modulate SAT variation by causing temporary local anomalies in the temperature advection. In particular, East Asia experiences frequent extratropical cyclones (ETCs) (Adachi and Kimura 2007; Zhang et al. 2012; Chen et al. 2014; Lee et al. 2020) as a result of its proximity to the location of the climatological maximum of the warm conveyor belt (Madonna et al. 2014), as well as high wave activity in the upper level of the region (Chang et al. 2002; Hoskins and Hodges 2002; Madonna et al. 2014). Furthermore, synoptic-scale transient eddy activity and baroclinic instability, which play a role in the generation of ETCs, are most pronounced in the spring (Ren et al. 2010). Therefore, ETC activity in East Asia is most active in the spring, compared to other seasons (Wang et al. 2009; Kim et al. 2021), indicating they can contribute significantly to SAT variation. Consequently, this study includes an analysis of their impact on spring SAT variations over East Asia.

A variety of methods to detect migratory pressure systems have been developed and utilized, some of which are based on the SLP filed (Adachi and Kimura 2007; Zhang et al. 2012). However, the SLP-based approach is mostly useful for vertically well-developed systems, but is less effective in the early stages of system development (Sinclair 1997; Hodges 1999). For complex terrain with mountain ranges and plateaus like the terrain in East Asia, SLP is calculated by vertical extrapolation, which introduces considerable error (Sinclair 1997; Hodges 1999; Hoskins and Hodges 2002). To avoid this, researchers have used relative vorticity at 850 hPa instead of SLP in recent studies of the ETC, such as Chen et al. (2014), Kang et al. (2020), and Lee et al. (2020). Compared to SLP, relative vorticity at 850 hPa is more efficient when focusing on smaller spatial scales, and is less affected by background, making it easier to identify synoptic tracks (Mailier et al. 2006).

Our study followed the method proposed by Hodges (1994, 1995, 1999), which uses six-hour relative vorticity at 850 hPa to identify and track migratory pressure systems. In order to focus on synoptic-scale ETCs, relative vorticity is spectrally truncated to a T42 spectral resolution (approximately 2.8° of latitude), and waves with wavenumbers less than 5 were masked to remove the influence of planetary-scale waves. Then, the Connected Component Labeling Algorithm (Rosenfeld 1976) was employed to separate individual vorticity features from the background, and the centers of selected migratory pressure systems were tracked at six-hour intervals based on specific criteria. Further details can be found in Hodges (1994, 1995, 1999), and the final conditions were as follows: (1) occurrence at latitudes above 25°N, (2) lifetime of at least two days, (3) a trajectory of more than 1000 km, and (4) center intensity greater than $1.0\times10^{-5}\ s^{-1}$ for ETCs, or less than $-1.0\times10^{-5}\ s^{-1}$ for migratory anticyclones (Hoskins and Hodges 2002; Kang et al. 2020; Lee et al. 2020).

2.3 Climate indices

For this study, regression analysis was used to estimate the effects of atmospheric circulation and global warming on SAT variation for East Asia. This method was utilized in previous studies like Kim et al. (2022) because it is simple and efficient in explaining the relationship between variables. Therefore, various atmospheric circulation indices were collected in order to select one that is closely related to the March DTV, which showed a significant increasing trend for 42 years, as detailed in Sect. 3 below.

The East Asian monsoon climate is strongly dominated by planetary-scale circulation characterized by the Siberian High (SH), the Aleutian Low (AL), the East Asian Trough (EAT), and the East Asian jet stream (EAJS) during the winter (Ha et al. 2012), and these systems persist until early boreal spring. The details of the four East Asian winter monsoon (EAWM) indices are summarized in Table 1. Because each index represents a major component of the EAWM system and has a strong correlation with the East

Table 1 Description of the East Asian winter monsoon (EAWM) indices used in this study

Name	Definition	Reference
Siberian High (SH)	The area-averaged sea-level pressure for the region (40°–60°N, 70°–120°E)	Gong et al. (2001)
Aleutian Low (AL)	The area-averaged sea-level pressure for the region (45°–65°N, 160°E-160°W)	Sun et al. (2019)
East Asian Trough (EAT)	The area-averaged 500 hPa geopotential height for the region (30°–45°N, 125°–145°E)	Sun and Li (1997)
East Asian jet stream (EAJS)	The difference in the area-averaged zonal wind speed at 300 hPa between the two regions: (27.5°–37.5°N, 110°–170°E) − (50°–60°N, 80°–140°E)	Jhun and Lee (2004)

Asian SAT, they have been widely used in EAWM-related studies (e.g., Ha et al. 2012; Shin and Moon 2018; Miao and Wang 2020). In the study, the AL index was replaced by the spring AL index defined by Sun et al. (2019) to consider its northward retreat with the seasonal transitions. A strong EAWM is expressed by positive values for the SH and EAJS indices and negative values for the AL and EAT indices. Additionally, seven teleconnection and atmospheric circulation indices known to influence the East Asian SAT during the cold season (Kim et al. 2017) were used in this study. They are the Pacific/North American (PNA), North Atlantic Oscillation (NAO), Western Pacific (WP), East Atlantic (EA), Scandinavia (SCAND), Eastern Asia/Western Russia (EA/WR), and Arctic Oscillation (AO) indices, which can be obtained from the NOAA Climate Prediction Center (CPC) website (https://www.cpc.ncep.noaa.gov/data/teledoc/telecontents.shtml).

2.4 Long-term global warming trend index

The long-term trend in global warming can be utilized as an index to examine the direct impact of global warming on SAT variations in East Asia. In this study, the long-term global warming trend (GWT) index is defined as the 42-year linear trend of the global mean 500 hPa GPH. The slope of the global mean SAT is sensitive to the period of interest; for example, the warming rate for 1998–2012, which contained a strong El Niño, was slower (0.05 °C/10 years) than for 1951–2012 (0.12 °C/10 years) (IPCC 2014). In contrast, the global mean 500 hPa GPH thermally contracts or expands with the mean temperature in the lower troposphere, making it a suitable variable to provide information on changes in the atmospheric thermal structure. In this regard, Christidis and Stott (2015) detected a substantial global increase in the annual and seasonal mean 500 hPa GPH by using four reanalysis datasets, and they evaluated them as reliable compared to the global mean SAT. Therefore, the GWT index is defined based on the global mean 500 hPa GPH to minimize under- or overestimation of the direct effect of global warming on SAT variation.

3 SAT variation during spring over East Asia

Figure 1 illustrates the climatology and 42-year linear trend of the spring DTV and monthly (March, April, and May) DTVs for the period 1979 to 2020. As shown in Fig. 1a, the spring DTV is less than 2.5 K over the ocean, 2.5-4 K over coastal areas such as southern and eastern China, the Korean Peninsula, and Japan, and up to 5.5 K inland. Each March, April, and May, the DTV is also greater over the land than over the ocean, and on land is relatively greater inland than over coastal areas (Fig. 1b–d). In brief, regardless of the timescale used to define the variation (e.g., seasonal or monthly), the climatological DTV increased as the ocean influence decreased, similar to the findings of Babina and Semenov (2019). Furthermore, the DTV decreased over time from March to May, with the decrease being greater over land than over the ocean and at higher latitudes than at mid-latitudes. Hence, these features led to high DTVs above 6 K in March at high latitudes above 60°N.

As for the long-term trend, DTV for the entire spring season decreased over the 42-year period, but was not statistically significant (see Fig. 1a), whereas the DTV for one month varied from month to month (see Fig. 1b–d). Both the March and April DTVs tended to increase in East Asia, with a statistically significant and relatively large increase in March. Meanwhile, the May DTV showed a decreasing trend in southern China and east of Lake Baikal, which partially offsets the increasing trend in March and April, making the spring DTV trend insignificant. Furthermore, additional analyses of other seasons and months showed no significant changes over the 42-year period (see Figs. S1–S3), and these features are also evident in the observations from the BEST dataset (Fig. S4).

This long-term trend of an increasing March DTV is not sufficiently explained by the prevailing hypothesis of Arctic amplification under global warming. In order to analyze the mechanisms involved, the DTV averaged from the boxed area of Fig. 1b is denoted DTV_EA, and subsequent analyses were performed using it. Figure 2 presents its time series and the long-term trend from 1979 to 2020, where DTV_EA above 6 K is observed in the final decade.

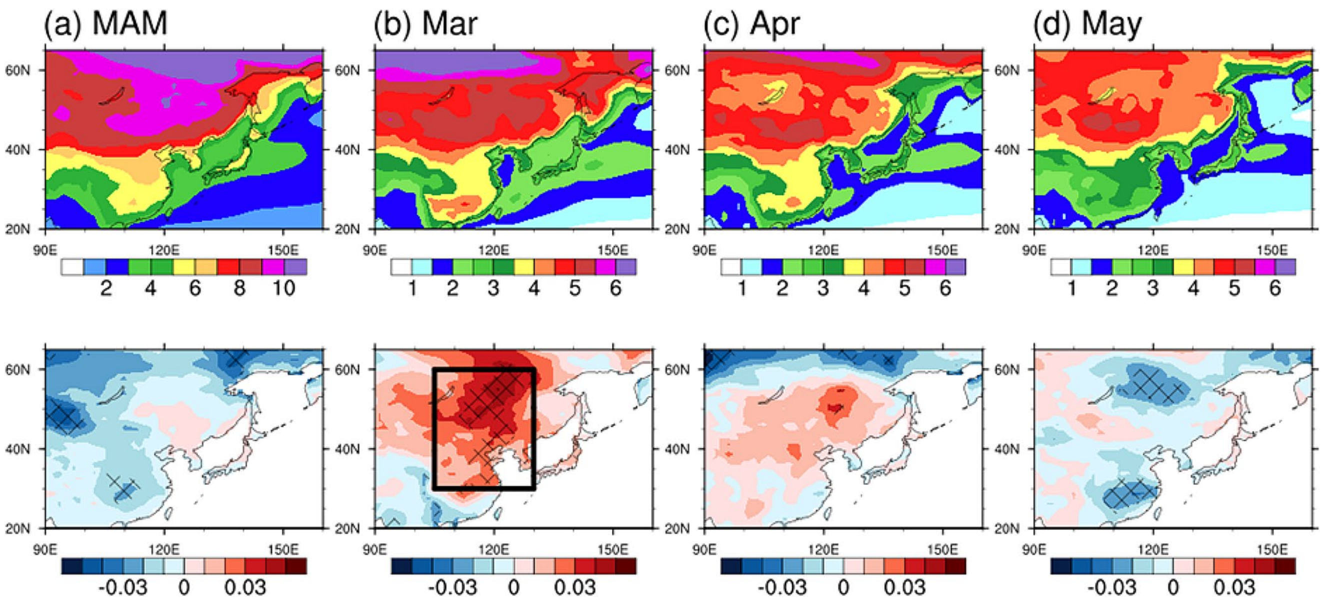

Fig. 1 (Top) climatology and (bottom) linear trends of daily temperature variation (DTV) during 1979–2020 for **a** March to May, **b** March, **c** April, and **d** May. Thin nets are significant at the 95% confidence level; the box indicates the region used to define DTV over East Asia (DTV_EA) for March

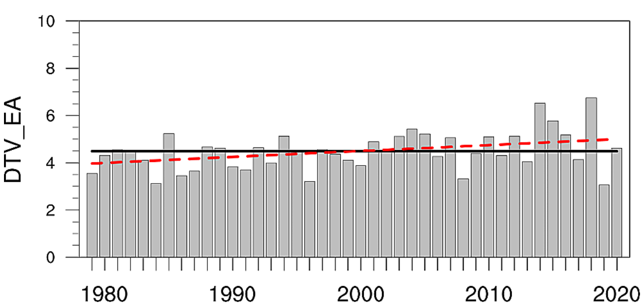

Fig. 2 Time series of the DTV_EA for March from 1979 to 2020, and its (solid line) average and (dashed line) trend over 42 years

Table 2 Years in which March DTV_EA was greater than +1 standard deviation or less than −1 standard deviation from 1979 to 2020. In this study, the former is defined as Above Years (AYs) and the latter as Below Years (BYs)

	Years
Above Years (> +1σ)	1985, 2004, 2014, 2015, 2018
Below Years (< −1σ)	1984, 1996, 2008, 2013, 2017, 2019

4 Climate processes affecting the March DTV over East Asia

4.1 Large-scale atmospheric circulation

In this study, a composite analysis is carried out to investigate the climatic processes affecting the March DTV. This method shows the response of the surrounding regions in relation to the phenomenon of interest, proving crucial information needed to formulate hypotheses that can explain the relationship among them (Boschat et al. 2016). For the analysis, Above Years (AYs) and Below Years (BYs), respectively, are defined as years that deviate by +1 and −1 standard deviation in the 42 years of the DTV_EA time series (Table 2). We detrended all variables to remove some of the effects of global warming, especially those associated with linear changes in each variable.

Figure 3 shows composite maps for each climate variable in the surface layers and upper troposphere during AYs and BYs, and the differences between them. Here, the noticeable differences between AYs and BYs reveal that the March DTV in East Asia is associated with a large-scale atmospheric circulation. For AYs, the DTV anomaly is positive over the mid-latitudes of the Eurasian continent, especially +2 K or more southeast of Lake Baikal (Fig. 3a). As shown in Fig. 3b, the spatial pattern of the composite SLP consists of a positive anomaly in the North Pacific and a negative anomaly over Russia, with the positive anomaly being relatively more distinct. The anomalies are negligible southwest of Lake Baikal, the climatological location of the SH, suggesting a weak connection to the March DTV in East Asia. Meanwhile, much of the region near the Aleutian Islands, where the center of the AL is climatologically located, has positive anomalies due to the anomaly in the North Pacific. As one of the main components of the EAWM system, the AL is active from late autumn to late spring, and retreats towards the Arctic as the subtropical high dominates the North Pacific during the summer (Pickart et al. 2009; Sun et al. 2019). Therefore, the positive anomaly located south of

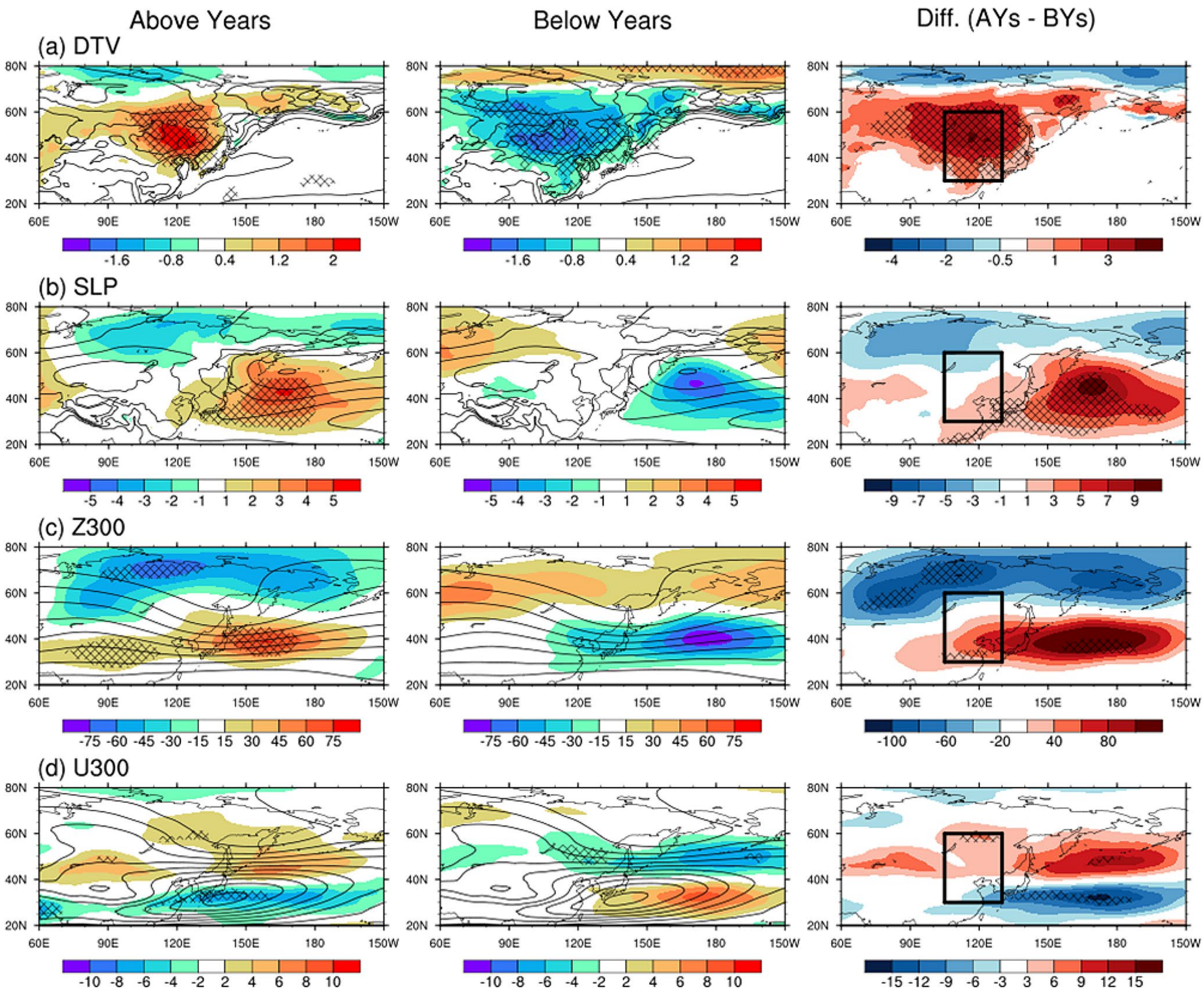

Fig. 3 Composite maps of detrended anomalies in **a** DTV, **b** sea level pressure, **c** 300 hPa geopotential height, and **d** 300 hPa zonal wind in March for (left) AYs, (center) BYs, and (right) the difference. The contour lines in the left and center columns represent climatology from 1979 to 2020, and the boxes in the right column indicate the region for the DTV_EA. Thin nets indicate significance at the 95% confidence level

the AL center during the AYs can be interpreted as a faster-than-normal AL retreat associated with the seasonal change. This pattern of anomalies over East Asia is also evident in the 300 hPa GPH, indicating that the anomalies have a vertically developed structure from the lower to upper troposphere (Fig. 3c). In particular, the positive GPH anomaly in the North Pacific induces an anomalous anticyclonic circulation in the region, which weakens the 300 hPa zonal wind at 20°–40°N (i.e., a negative anomaly), but strengthens at 40–50°N (i.e., a positive anomaly) (Fig. 3d). This eventually suggests a weakening of the EAJS during the AYs.

In contrast, the anomalous patterns in SLP and 300 hPa GPH for the BYs consist of a negative anomaly in the North Pacific and a positive anomaly over Russia. The negative anomaly represents a southward extension or development of the AL during the BYs, implying persistence of a strong AL influence into March. As a result of these anomalous GPH patterns, anomalous cyclonic circulation in the North Pacific led to an intensification of the EAJS at 300 hPa.

To explore the relationship between the atmospheric conditions shown in Fig. 3 and the March DTV in East Asia, we further examined the GPH and horizontal winds in the lower troposphere and the monthly mean SAT (Fig. 4). During the AYs, the composite map for the 850 hPa GPH consists of a positive anomaly in the North Pacific and a negative anomaly over Russia (Fig. 4a), similar to the SLP in Fig. 3b and the 300 hPa GPH in Fig. 3c. As shown in Fig. 4b, the anomalous anticyclonic circulation caused by the positive GPH anomaly in the North Pacific brings warm air from the subtropical North Pacific over eastern China, the Korean

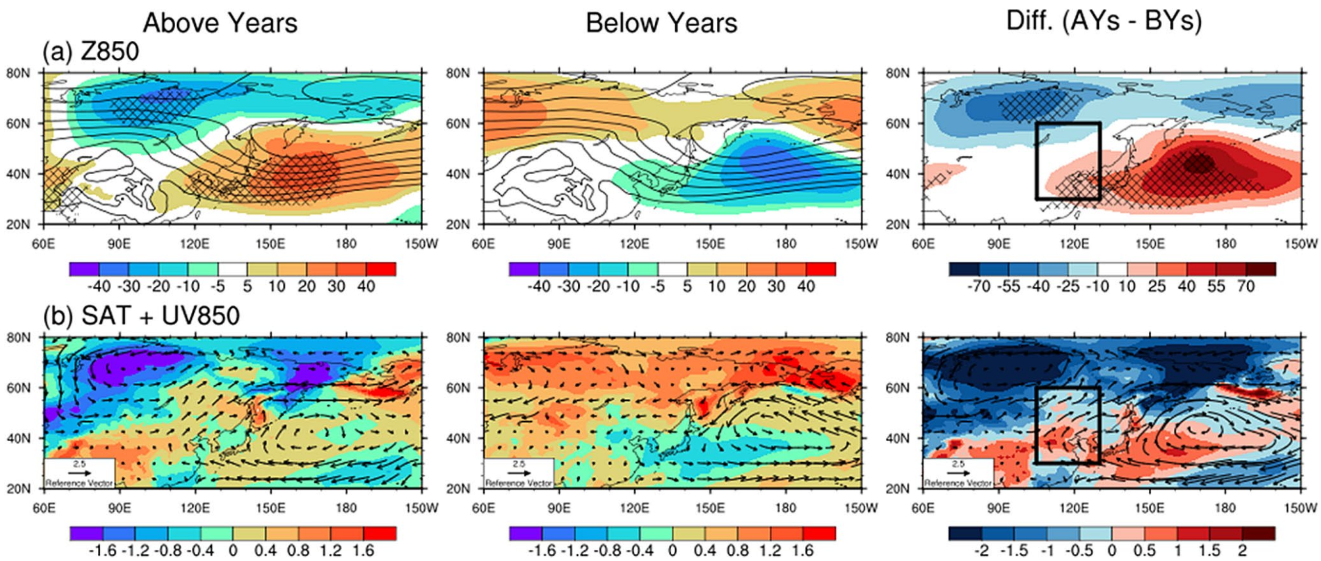

Fig. 4 Composite maps of detrended anomalies in **a** 850 hPa geopotential height and **b** monthly surface air temperature (shading) and 850 hPa horizontal wind (vectors) in March for (left) AYs, (center) BYs, and (right) the difference. In **a**, the contour lines represent climatology from 1979 to 2020 and thin nets indicate significance at the 95% confidence level. The boxes in the right column indicate the region for the DTV_EA

Peninsula, and Japan. Meanwhile, the anomalous cyclonic circulation caused by the negative GPH anomaly over Russia transports cold Arctic air into the Eurasian continent, especially at 60°E. Additionally, the two GPH anomalies drive strong northeastward wind anomalies over Manchuria, which is located in between. In other words, the anomalous circulations during AYs make Manchuria, eastern China, the Korean Peninsula, and Japan warmer than normal, and make Russia colder. As a result, the meridional gradient of the SAT increases regionally at around 50°N due to colder conditions in the north and warmer conditions in the south. This makes the environment more susceptible to drastic temperature changes, resulting in a greater than normal March DTV.

On the other hand, the 850 hPa GPH anomaly pattern for BYs is the opposite of AYs, with a negative anomaly in the North Pacific and a positive anomaly over Russia. Here, the negative GPH anomaly in the North Pacific transports cold air from the Bering Sea and the Sea of Okhotsk through southwestward wind anomalies into eastern China, the Korean Peninsula, and Japan. The positive anomaly over Russia also induces strong eastward wind anomalies near 70°–80°N that prevent cold Arctic air from moving south and bring relatively warm air from the Atlantic Ocean to the continent. As a result, a widespread warm anomaly appears over the Eurasian continent, while a cold anomaly occurs over eastern China, the Korean Peninsula, Japan, and some areas of the northwestern Pacific. This reduces the meridional SAT gradient over the Eurasian continent, ultimately leading to a decrease in DTV compared to normal years.

4.2 Migratory pressure system

The potential impact of synoptic-scale pressure system activity on the March DTV in East Asia is further studied in Fig. 5 and S5. Figure 5 shows composites of the ETC frequency anomaly during AYs and BYs, where the ETC frequency is the number of ETCs that pass through each grid point during March. If the same ETC was detected multiple times at a grid point, it was counted only once. For AYs (Fig. 5a), the positive ETC frequency anomaly for 50°–65°N overlaps with the region where the meridional gradient of the SAT increased due to anomalous atmospheric circulation (see Fig. 4b). Considering that ETCs are mainly caused by conversion of potential energy from the meridional temperature gradient into eddy kinetic energy (Okajima et al. 2021), we can infer that the enhanced meridional SAT gradient contributed positively to the activities of ETCs. Meanwhile, the negative anomaly of the ETC frequency over Manchuria in Fig. 5a is related to strong northward wind anomalies that prevent ETCs from entering the region (see Fig. 4b). Additionally, the ETCs play a role in maintaining the thermal structure and mid-latitude westerly jet stream by systematically transporting heat and momentum (Okajima et al. 2021). In this regard, in Fig. 3d, an upper-level westerly anomaly appears to the north of the Tibetan Plateau where the East Asian polar jet (EAPJ) is climatologically located. On the other hand, during BYs (Fig. 5b), ETC activity is lower than normal across the Eurasian continent, with an anomaly of about −1.6 over Russia. This is related to the weakening of the meridional SAT gradient and the westward 850 hPa wind anomalies shown over the region in

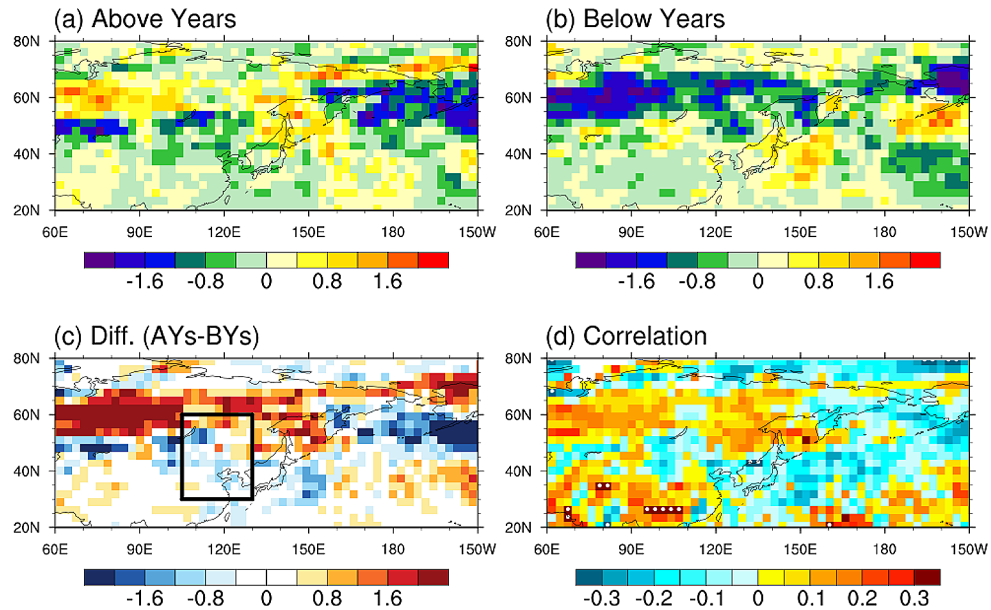

Fig. 5 Anomalies in track density for the extratropical cyclone in March for **a** AYs, **b** BYs, **c** the difference between them, and **d** the spatial field of the correlation coefficient between track density and the DTV_EA. The box in **c** indicates the area of the DTV_EA. The white dots in **d** indicate significance at the 95% confidence level

Fig. 4b. The former may suppress the generation and development of ETCs, while the latter may impede their eastward propagation. Furthermore, the upper-level zonal wind shows westward anomalies north of the Tibetan Plateau, resulting in a weaker-than-normal EAPJ. Moreover, the composite result for the migratory anticyclone also shows more frequent passage over East Asia in the AYs than in the BYs (Fig. S5) influenced by anomalous eastward wind that appear at 40°–50°N during AYs.

The previous results demonstrate that March DTV in East Asia tends to be larger than normal under climatic conditions where migratory pressure systems are generally more active than normal (Fig. 5a-c). Although this relationship is not statistically significant (Fig. 5d), the difference in ETC activity during AYs and BYs may be physically important with respect to thermal advection, considering the enhancing SAT gradient in East Asia during AYs. Therefore, we examined the changes in regional temperature advection and analyzed the relationship with March DTV in East Asia. Figure 6 shows the difference in mean warm and cold advection between AYs and BYs, using only land grid points since the difference in the DTV is smaller over the ocean than over the land. Because warm (cold) advection is a positive (negative) value, a positive (negative) value on the x-axis (y-axis) indicates stronger warm (cold) advection during AYs than during BYs. In other words, a dot in the fourth (second) quadrant represents a grid point where both warm and cold advection is stronger (weaker). Comparing the difference in temperature advection between BYs and AYs showed that 39.6% of the grid points in East Asia experienced an increase in both warm and cold advection, and 38.3% of the grid points experienced an increase in either warm or cold advection alone (Table 3). Furthermore, the color of the dots indicates the DTV difference, and the majority of the dots in the fourth quadrant have values above 1.0, indicating the DTV increases more significantly for grid points with increased warm and cold advection. In conclusion, the enhanced SAT gradient and active migratory pressure systems over East Asia can contribute to the increase in March DTV by causing locally transient temperature advection anomalies.

4.3 Simultaneous correlation with climate indices

The previous composite analysis showed that the March DTV in East Asia is closely related to the surrounding atmospheric circulation. Since the results of composite analyses do not always imply a physical relationship, however, additional statistical analyses should be made to confirm the analyzed results (Boschat et al. 2016). In this section, we estimate simultaneous correlations between the March DTV_EA (the area-averaged value) and various EAWM and climate indices from 1979 to 2020. Prior to calculating the correlation coefficients, long-term linear trends were removed from both the DTV_EA and all indices.

Among the four EAWM indices, the March DTV_EA showed significant negative and positive correlations with the EAJS and EAT indices, respectively (Table 4). This can be explained by the negative zonal wind anomaly in the EAJS core (20°–40°N, 110°–170°E) as shown in Fig. 3d, and the positive 500 hPa GPH anomaly in the EAT (30°–45°N, 125°–145°E), as shown in Fig. S6 during the AYs (opposite to the pattern in BYs). On the other hand, the SH index had a correlation coefficient close to zero with the DTV_EA, indicating the relationship is nearly independent. This is related to the lack of a distinct SLP anomaly

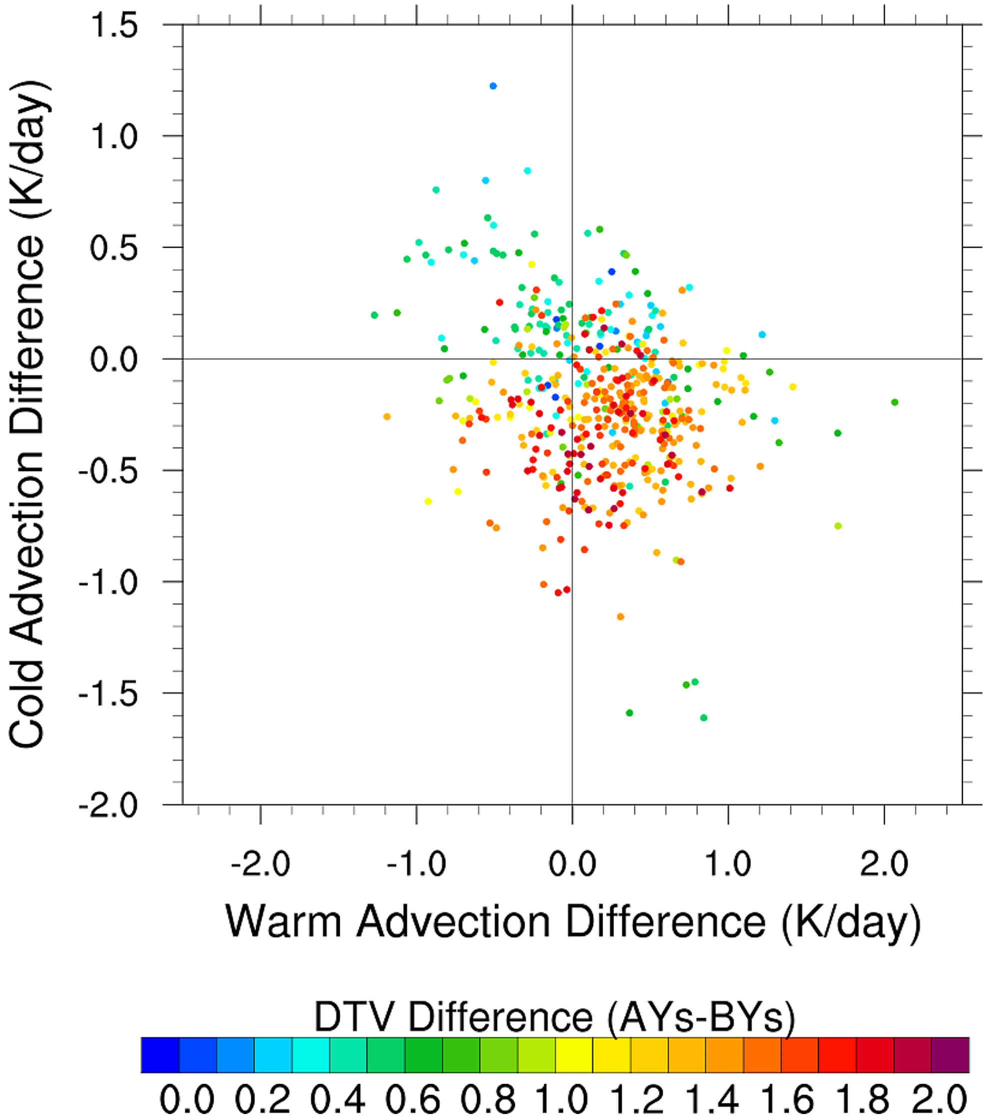

Fig. 6 Differences in 1000 hPa temperature advection for March between BYs and AYs at land grids in East Asia (30°–60°N, 105°–130°E). The color bar shows the differences in DTV, and positive (negative) values on the x-axis (y-axis) indicate intensification of warm (cold) advection

Table 3 Number of grid points from differences in 1000 hPa temperature advection for March over East Asia between BYs and AYs. Only land grid points are used

Difference (AYs – BYs)		Warm advection			
		Increase	No change	Decrease	Total
Cold advection	Increase	964	87	429	1,480
	No change	20	0	63	83
	Decrease	397	12	463	872
	Total	1,381	99	955	2,435

Table 4 Correlation coefficients between DTV_EA and climate indices for March from 1979 to 2020

EAWM indices	Correlation coefficients	Other indices	Correlation coefficients
SH	0.021	PNA	-0.108
AL	0.289	NAO	-0.030
EAT	0.317*	WP	0.148
EAJS	-0.403**	EA	0.208
		SCAND (EU1)	0.009
		EA/WR (EU2)	0.306*
		AO	0.077

The indices used are four EAWM indices and seven Northern Hemisphere winter atmospheric teleconnection indices (including AO)

* and ** indicate significance at the 95% and 99% confidence levels, respectively. All variables were detrended prior to calculation

in the region of SH during AYs and BYs (see Fig. 3b). Furthermore, the SLP anomaly in the North Pacific that affects the March DTV includes only a southern part of the AL, as illustrated in Fig. 3b, so the correlation coefficient between DTV_EA and the AL index is positive, although not statistically significant. In summary, the March DTV in East Asia is independent of the SH index but correlates positively with the AL and EAT indices and correlates negatively with the EAJS index. In short, the March DTV in East Asia tends to be larger when the overall EAWM system is weaker.

When examining the correlations with various climate indices influencing the SAT during the cold season in East Asia, only the EA/WR index showed a significant positive correlation (see Table 4). The EA/WR pattern, a major planetary-scale circulation pattern occurring in the eastern Atlantic, consists of two major large-scale anomalies in the Caspian Sea and western Europe, which propagate eastward to affect the mid-latitude continent of Asia (Barnston and Livezey 1987). In this regard, Lim (2015) mentioned that the wave structure of the EA/WR pattern can lead to alternating periods of locally warm and cold weather through anomalies in atmospheric circulation and temperature advection. Furthermore, according to Lim and Kim (2013), who studied temperature and atmospheric circulation anomalies associated with the EA/WR teleconnection, the positive phase of the EA/WR pattern causes negative SAT anomalies over Russia and positive SAT anomalies over East Asia. This generates a strong cyclonic circulation anomaly over western Russia and an anticyclonic circulation anomaly over East Asia and the North Pacific in the lower troposphere while weakening the EAJS in the upper troposphere. These key features resemble the composite results for AYs in Figs. 3 and 4, and the EA/WR index also showed a strong negative correlation coefficient of -0.72 with the EAJS index. These results indicate that the EAJS index can represent the atmospheric circulation affecting the March DTV in East Asia.

5 Contribution estimation based on regression analysis

In this section, we quantitatively evaluate the contribution of atmospheric circulation and global warming to the East Asian March DTV by using regression analysis. Figure 7 presents a time series of regression results for the DTV_EA and the independent variables used in each regression analysis. The upper row shows the results of linear regression on the DTV_EA using the detrended EAJS index, and the lower row shows the results of adding the GWT index as an independent variable. Since the EAJS index had a weak declining trend at the 90% significance level from 1979 to 2020 (Fig. S7a), the long-term trend was removed to ensure the statistical independence of the independent variables in the multiple regression analysis. Details of the GWT index are described in Sect. 2.4. The correlation coefficients between the observed DTV_EA and the two regression results are 0.37 and 0.53, and 0.12 and 0.24 for the adjusted coefficients of determination. Including the GWT index improves agreement with the observations, suggesting that the long-term trend in global warming contributes to the increase in March DTV in East Asia.

Figure 8 is the correlation coefficient maps between the regression results and observations in order to examine the spatial influence of the EAWM and GWT on the March DTV in East Asia. The linear regression results with the detrended EAJS index alone showed relatively high correlation coefficients of up to 0.5 centered on Lake Baikal, while correlation coefficients below 0.2 were found over the Korean Peninsula and southern Japan (Fig. 8a). This is attributed to the changes in the meridional SAT gradient associated with the anomalous atmospheric circulation, which is more pronounced around Lake Baikal than over the Korean Peninsula and southern Japan. Meanwhile, as shown in Fig. 8b, the linear regression results using only the GWT index indicate

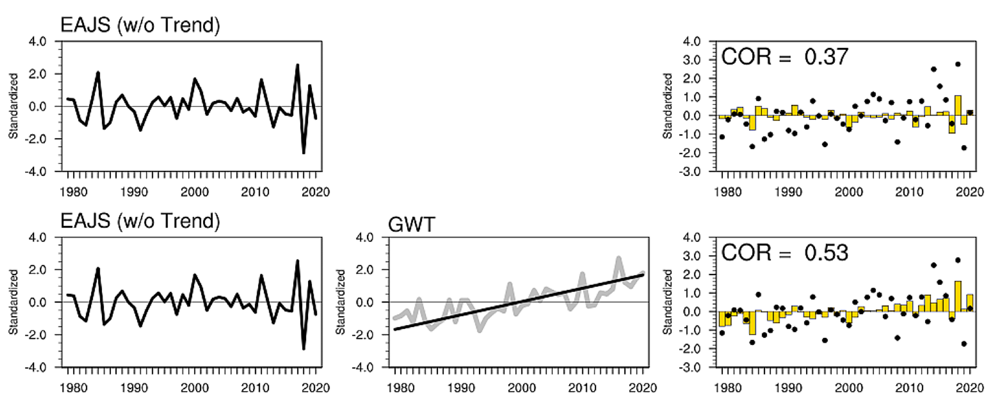

Fig. 7 Time series of the (left and center) standardized independent variables and (right) regression results for the DTV_EA in March from 1979 to 2020. The independent variable in the upper row is only the detrended EAJS index, and in the lower row, the long-term global warming trend (GWT) index is added as an independent variable. The GWT index is defined as the 42-year linear trend (black line) in the global-averaged 500 hPa geopotential height (gray line). In the right column, the dots are the standardized versions of the DTV_EA shown in Fig. 2, and 'COR' means correlation coefficient with the regression results

Fig. 8 Spatial maps of correlation coefficients of **a**, **b** linear and **c** multiple regression results with the observed March DTV during 1979–2020. Each predictor is **a** the detrended EAJS index, **b** the GWT index, and **c** both

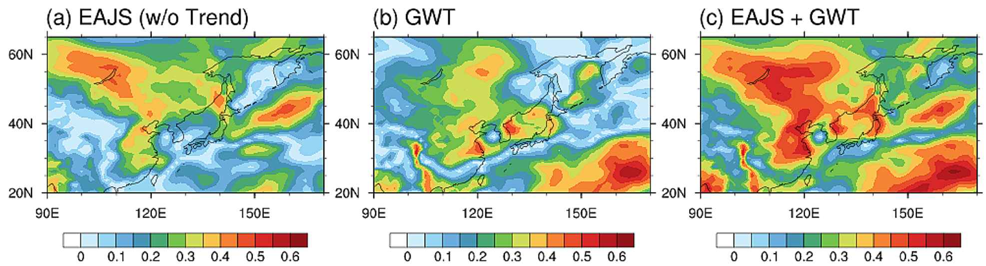

correlation coefficients that are relatively evenly distributed across East Asia (at least 0.3) except in local areas such as eastern China, the Korean Peninsula, and the adjacent sea. In the multiple linear regression analysis with both indices (Fig. 8c), the correlation coefficients generally ranged from 0.3 to 0.6 in the East Asian region, indicating higher values than when only one independent variable was considered. These results suggest that both atmospheric circulation and global warming should be considered for a clear understanding of the changes in March DTV in East Asia.

6 Discussion

6.1 The role of global warming

In this study, the global warming effect was represented through the GWT index, but the actual global warming effect varies depending on the period, region, and variables. Therefore, we discuss the role of global warming on March DTV from various aspects.

Although statistical independence of the EAWM and the GWT was assumed for the multiple regression analysis, this does not mean their physical relationship is also independent (Kim et al. 2022). The linear regression result considering the long-term trend in the EAJS (Fig. S7b) has a higher correlation coefficient with the observations (0.46) than when it is removed (0.37), suggesting that the weak declining trend in the EAJS can contribute to the increase in the DTV_EA. If the long-term weakening of the EAJS is partly due to global warming, it shows an indirect contribution from global warming to DTV. In this regard, various previous studies have demonstrated that the overall weakening of the EAWM systems has been attributed to global warming (Hori and Ueda 2006; Archer and Caldeira 2008; Song et al. 2019; Sun et al. 2019). The change in zonal mean SLP averaged in the North Pacific (160°–200°E) from 1979 to 2020 shows a steady increase, especially in the region of the AL (45°–65°N, 160°–200°E) (Fig. S8). This finding is similar to the results of Sun et al. (2019), who reported a significant weakening of the AL in spring. Therefore, the weakening of the EAWM system associated with global warming could partially contribute to the increase in March DTV over East Asia. However, in Fig. 8, the spatial patterns of the EAWM and GWT contributions are clearly different, suggesting the existence of a global warming role that is unrelated to the EAWM.

A reasonable hypothesis concerns spatially heterogeneous warming rates of the monthly mean SAT. Figure 9 shows the 42-year linear trends of monthly mean SAT and soil moisture for March and April. The March SAT shows a strong and significant trend above 0.08 K/year over eastern China, but in Manchuria, it is relatively weak (about 0.06 K/year) and not significant at the 95% confidence level (Fig. 9a). As a result, the meridional SAT gradient increases locally in the eastern region of Lake Baikal, ultimately making it favorable for the DTV to increase. This could be the reason for the relative concentration of the GWT contribution in the region, as shown in Fig. 8b. Additionally, while the warming signal is negligible in the Yellow Sea, the East Sea shows a warming of up to 0.06 K/year. Under these conditions, the daily SAT on the Korea Peninsula is more variable, depending on local changes in zonal wind.

Meanwhile, soil moisture can affect DTV by partitioning of the surface fluxes in intermediate moisture regimes. For example, low soil moisture conditions reduce evapotranspiration, which enhances sensible heat flux, and thus increases SAT. Because an increased SAT makes the soil drier, a decrease in soil moisture ultimately leads to a short-term increase in SAT. For detailed information on soil moisture-temperature feedback, see Seneviratne et al. (2010). Moreover, based on the CMIP5 models, Bathiany et al. (2018) suggested that the increased DTV is partially associated with decreased soil moisture. In this respect, the significant localized decrease in soil moisture associated with global warming could partially contribute to the increase in March DTV in East Asia over the 42-year period (Fig. 9b).

6.2 The unique features of March

The significant and strong increase in DTV is observed only in March, as shown in Fig. 1, which raises the question, What makes March unique? To discuss this, we conducted additional research on April, which shows a weak increasing trend in DTV (not statistically significant), and compared it with March. This suggested that the change in March DTV

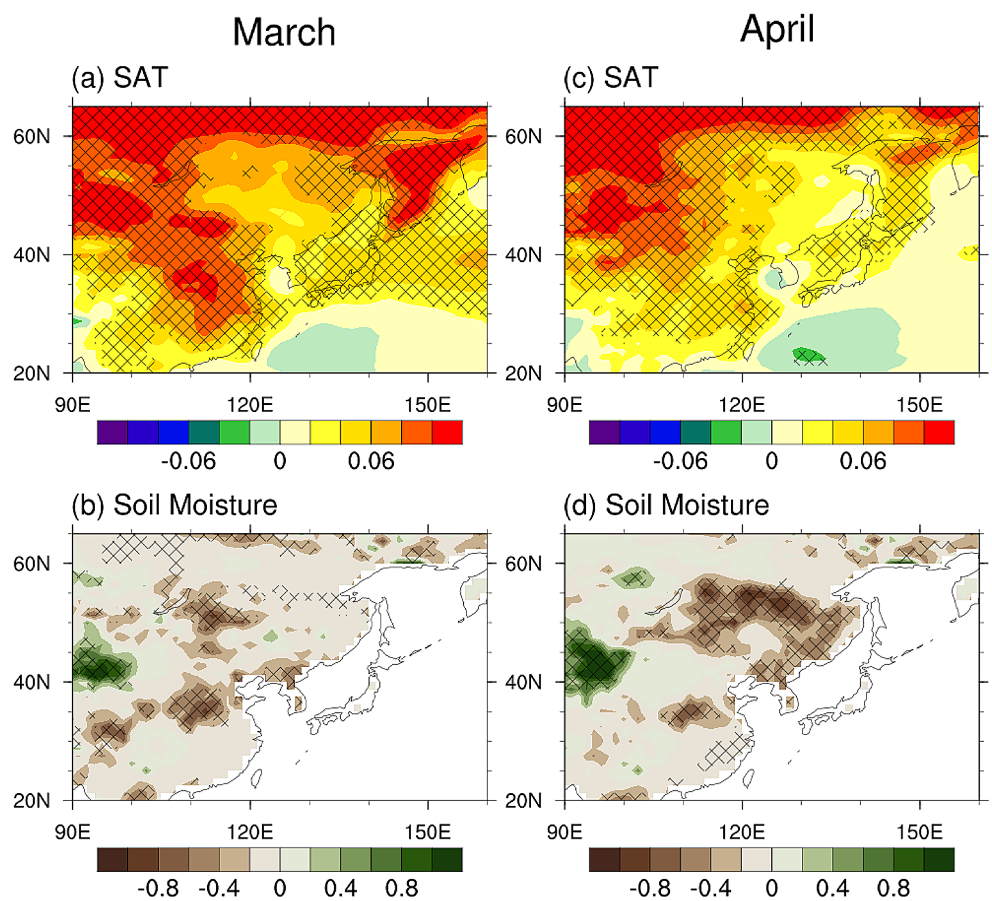

Fig. 9 Linear trends from 1979 to 2020 of **a**, **c** monthly surface air temperature and **b**, **d** soil moisture in **a**, **b** March and **c**, **d** April. Thin nets indicate significance at the 95% confidence level

is associated with the EAWM (especially the EAJS), heterogeneous warming rates, and a decrease in soil moisture. From this perspective, the East Asian climate in April is no longer affected by the EAWM, and even the April EAJS index has not changed significantly in 42 years (Fig. S9a). Moreover, the strong warming trend over eastern China in March does not appear in April, and the warming rates are faster at high latitudes compared to mid-latitudes, weakening the meridional SAT gradient (Fig. 9c). In contrast, soil moisture tends to decrease significantly in Manchuria (Fig. 9d), which is associated with decreased precipitation in the region (Fig. S9b). Considering that the April DTV has an increasing trend in the region (Fig. 1c), we can conclude that unlike March, the April DTV is mainly determined by soil moisture changes. This suggests that the increase in the March DTV is the result of a combination of unique conditions in March related to atmospheric circulation changes and global warming.

7 Summary and conclusion

It is important to understand how SAT variation will change under global warming, as well as the mechanisms involved. In general, a decreasing trend in SAT variation associated with Arctic amplification has been reported in the mid- and high latitudes of the Northern Hemisphere. However, increasing trends in SAT variation were also observed in some regions and during some seasons, suggesting that SAT may become more variable in these regions in the future. Changes in spring SAT variation can be directly related to the quantity and quality of agricultural production during the year in terms of crop germination and fruit development, although most previous studies have focused on the summer and winter. The purpose of this study is ultimately to understand the changes in spring SAT variation in East Asia during the 1979–2020 period. Observational and reanalysis data showed that the March DTV increased significantly over that 42-year period, while other spring SAT variations did not exhibit significant changes. Therefore, we identified the atmospheric circulation associated with the March DTV and examined its impact on the March DTV with global warming.

According to the composite analysis, the climate patterns in East Asia in years with above-normal March DTV were generally the opposite of those in years with below-normal DTV. The climatic features associated with above-normal March DTV included positive SLP anomalies in the North Pacific and negative SLP anomalies over Russia, which bring subtropical warm air and Arctic cold air, respectively, to inland East Asia in the lower troposphere. This leads to an increase in the meridional SAT gradient in East Asia, which is conducive to an increase in March DTV. These circulation anomalies are similar in the upper troposphere, and those in the North Pacific weaken the EAJS by causing westward anomalies in the core region of the EAJS (20°–40°N, 110°–170°E). In addition, March DTV tends to be larger than normal as more migratory pressure systems pass over East Asia. This could lead to stronger transient temperature advection anomalies under the enhanced meridional SAT gradient due to anomalous atmospheric circulation.

Simultaneous correlation analysis of the East Asian March DTV with various EAWM and climate indices generally indicated that a weaker EAWM system was associated with greater DTV, supporting the previous composite analysis. Although the SH index was not significantly correlated, the AL and EAT indices correlated positively, and the EAJS index correlated significantly and negatively at the 99% confidence level. Moreover, the EA/WR index was the only significant correlation among the seven climate indices. The temperature and atmospheric circulation anomalies associated with the positive phase of the EA/WR teleconnection included the main climatic features of the year in which the March DTV in East Asia was above normal.

Regression analysis was used to examine the impact of the EAWM and global warming on March DTV in East Asia. The results showed that both factors significantly contributed to March DTV from 1979 to 2020. Spatially, the impact of the EAJS on March DTV was relatively concentrated in the inland regions around Lake Baikal, while the GWT was evenly distributed across East Asia, except for a few regions. These differences in spatial patterns imply that global warming affects the March DTV separately from the EAWM. In this respect, the role of global warming is likely related to heterogeneous warming rates and localized soil drying in East Asia during the study period.

We examined spring SAT variations and found a unique increasing trend in March DTV, which is a result of significant effects from atmospheric circulation (i.e., EAWM) and global warming. These results suggest that further regional studies should be conducted to ensure a sustainability, as the effects of atmospheric circulation and global warming on SAT variation vary regionally and temporally.

Supplementary Information The online version contains supplementary material available at https://doi.org/10.1007/s00382-024-07129-x.

Author contributions Both authors contributed to the study conception and design. Material preparation, data collection and analysis were performed by S-HK. The first draft of the manuscript was written by S-HK and both authors commented on previous versions of the manuscript. Both authors read and approved the final manuscript.

Funding This work was carried out with the support of the "Cooperative Research Program for Agriculture Science and Technology Development (Project No. PJ01475503)", Rural Development Administration, Republic of Korea.

Data availability The monthly mean data in the JRA-55 dataset are available at https://rda.ucar.edu/datasets/ds628-1/ (accessed on 18 August 2023) and the 6-hourly data at https://rda.ucar.edu/datasets/ds628-0/ (accessed on 18 August 2023). The BEST datasets can be downloaded at https://berkeleyearth.org/data/ (accessed on 18 August 2023). The climate indices are provided at https://www.cpc.ncep.noaa.gov/data/teledoc/telecontents.shtml (accessed on 18 August 2023). Data analysis and graphics were conducted using the NCAR command language (NCL) (https://www.ncl.ucar.edu; accessed on 18 August 2023). The data generated during the current study are available from the corresponding author on reasonable request.

Declarations

Competing interests The authors declare that they have no conflict of interest.

References

Adachi S, Kimura F (2007) A 36-year climatology of surface cyclogenesis in East Asia using high-resolution reanalysis data. Sci Online Lett Atmos 3:113–116. https://doi.org/10.2151/sola.2007-029

Archer CL, Caldeira K (2008) Historical trends in the jet streams. Geophys Res Lett 35(8):L08803. https://doi.org/10.1029/2008GL033614

Babina ED, Semenov VA (2019) Intramonthly variability of daily surface air temperature in Russia in 1970–2015. Russ Meteorol Hydrol 44(8):513–522. https://doi.org/10.3103/S1068373919080028

Barnston AG, Livezey RE (1987) Classification, seasonality and persistence of low-frequency atmospheric circulation patterns. Mon Weather Rev 115:1083–1126. https://doi.org/10.1175/1520-0493(1987)115<1083:CSAPOL>2.0.CO;2

Bathiany S, Dakos V, Scheffer M, Lenton TM (2018) Climate models predict increasing temperature variability in poor countries. Sci Adv 4(5):eaar5809. https://doi.org/10.1126/sciadv.aar5809

Boschat G, Simmonds I, Purich A, Cowan T, Pezza AB (2016) On the use of composite analyses to form physical hypotheses: an example from heat wave – SST associations. Sci Rep 6:29599. https://doi.org/10.1038/srep29599

Chang EKM, Lee S, Swanson KL (2002) Storm track dynamics. J Clim 15(16):2163–2183. https://doi.org/10.1175/1520-0442(2002)015<02163:STD>2.0.CO;2

Chen L, Tan B, Kvamstø NG, Johannessen OM (2014) Wintertime cyclone/anticyclone activity over China and its relation to upper tropospheric jets. Tel-lus A 66:21889. https://doi.org/10.3402/tellusa.v66.21889

Chmielewski FM, Müller A, Bruns E (2004) Climate changes and trends in phenology of fruit trees and field crops in Germany, 1961–2000. Agric for Meteorol 121(1–2):69–78. https://doi.org/10.1016/S0168-1923(03)00161-8

Christidis N, Stott PA (2015) Changes in the geopotential height at 500 hPa under the influence of external climatic forcings. Geophys Res Lett 42:10798–10806. https://doi.org/10.1002/2015GL066669

Dione C, Lohou F, Chiriaco M, Lothon M, Bastin S, Baray JL, Yiou P, Colomb A (2017) The influence of synoptic circulations and local processes on temperature anomalies at three French observatories. J Appl Meteorol Climatology 56(1):141–158. https://doi.org/10.1175/JAMC-D-16-0113.1

Ebita A et al (2011) The Japanese 55-yearReanalysis JRA-55: an interim report. Sci Online Lett Atmos 7:149–152. https://doi.org/10.2151/sola.2011-038

Francis JA, Vavrus SJ (2012) Evidence linking Arctic amplification to extreme weather in mid-latitudes. Geophys Res Lett 39(6):L06801. https://doi.org/10.1029/2012GL051000

Gong DY, Ho CH (2004) Intra-seasonal variability of wintertime temperature over East Asia. Int J Climatol 24(2):131–144. https://doi.org/10.1002/joc.1006

Gong DY, Wang SW, Zhu JH (2001) East Asian winter monsoon and Arctic oscillation. Geophys Res Lett 28:2073–2076. https://doi.org/10.1029/2000GL012311

Gong H, Wang L, Chen W, Wu R (2021) Evolution of the east Asian winter land temperature trends during 1961–2018: role of internal variability and external forcing. Environ Res Lett 16(2):024015. https://doi.org/10.1088/1748-9326/abd586

Ha K-J, Heo K-Y, Lee S-S, Yun K-S, Jhun J-G (2012) Variability in the east Asian monsoon: a review. Met Apps 19(2):200–215. https://doi.org/10.1002/met.1320

Hodges KI (1994) A general method for tracking analysis and its application to meteorological data. Mon Weather Rev 122(11):2573–2586. https://doi.org/10.1175/1520-0493(1994)122<2573:AGMFTA>2.0.CO;2

Hodges KI (1995) Feature tracking on the unit sphere. Mon Weather Rev 123(12):3458–3465. https://doi.org/10.1175/1520-0493(1995)123<3458:FTOTUS>2.0.CO;2

Hodges KI (1999) Adaptive constrains for feature tracking. Mon Weather Rev 127(6):1362–1373. https://doi.org/10.1175/1520-0493(1999)127<1362:ACFFT>2.0.CO;2

Hori ME, Ueda H (2006) Impact of global warming on the east Asian winter monsoon as revealed by nine coupled atmosphere-ocean GCMs. Geophys Res Lett 33(3):L03713. https://doi.org/10.1029/2005GL024961

Hoskins BJ, Hodges KI (2002) New perspectives on the Northern Hemisphere Winter Storm Tracks. J Atmos Sci 59(6):1041–1061. https://doi.org/10.1175/1520-0469(2002)059<1041:NPOTNH>2.0.CO;2

IPCC (2014) In: Pachauri RK, Meyer LA (eds) Climate Change 2014: synthesis report. Contribution of Working groups I, II and III to the Fifth Assessment Report of the Intergovernmental Panel on Climate Change [Core writing Team. IPCC, Geneva, Switzerland, p 151

Jhun JG, Lee EJ (2004) A new east Asian winter monsoon index and associated characteristics of the winter monsoon. J Clim 17(4):711–726. https://doi.org/10.1175/1520-0442(2004)017<0711:ANEAWM>2.0.CO;2

JMA (2013a) JRA-55: Japanese 55-year Reanalysis, Daily 3-Hourly and 6-Hourly Data. Research Data Archive at the National Center for Atmospheric Research, Computational and Information Systems Laboratory. Dataset. https://doi.org/10.5065/D6HH6H41

JMA (2013b) JRA-55: Japanese 55-year Reanalysis, Monthly Means and Variances. Research Data Archive at the National Center for Atmospheric Research, Computational and Information Systems Laboratory. Dataset. https://doi.org/10.5065/D60G3H5B

Kang JM, Lee J, Son S-W, Kim J, Chen D (2020) The rapid intensification of east Asian cyclones around the Korean Peninsula and their surface impacts. J Geophys Res Atmos 125(2):e2019JD031632. https://doi.org/10.1029/2019JD031632

Katz RW, Brown BG (1992) Extreme events in a changing climate: variability is more important than averages. Clim Change 21:289–302. https://doi.org/10.1007/BF00139728

Kim ST, Sohn S-J, Kug J-S (2017) Winter temperatures over the Korean Peninsula and East Asia: development of a new index and its application to seasonal forecast. Clim Dyn 49:1567–1581. https://doi.org/10.1007/s00382-016-3402-2

Kim D, Lee J, Kang JM, Son S-W (2021) Synoptic structures and precipitation impact of extratropical cyclones influencing on East Asia megacities: Seoul, Beijing. Tokyo Atmos 31(1):45–60. https://doi.org/10.14191/ATMOS.2021.31.1.045(in Korean with English abstract)

Kim SH, Kryjov VN, Ahn JB (2022) The roles of global warming and Arctic Oscillation in the winter 2020 extremes in East Asia. Environ Res Lett 17(6):065010. https://doi.org/10.1088/1748-9326/ac7061

Kotz M, Wenz L, Stechemesser A, Kalkuhl M, Levermann A (2021) Day-to-day temperature variability reduces economic growth. Nat Clim Change 11(4):319–325. https://doi.org/10.1038/s41558-020-00985-5

Lee J, Son S-W, Cho H-O, Kim K, Gyakum CD-H, J. R., Chen D (2020) Extratropical cyclones over East Asia: climatology, seasonal cycle, and long-term trend. Clim Dyn 54:1131–1144. https://doi.org/10.1007/s00382-019-05048-w

Lim Y-K (2015) The East Atlantic/West Russia (EA/WR) teleconnection in the North Atlantic: climate impact and relation to Rossby wave propagation. Clim Dyn 44:3211–3222. https://doi.org/10.1007/s00382-014-2381-4

Lim Y-K, Kim H-D (2013) Impact of the dominant large-scale teleconnections on winter temperature variability over East Asia. J Geophys Res Atmos 118(14):7835–7848. https://doi.org/10.1002/jgrd.50462

Madonna E, Wernli H, Joos H, Martius O (2014) Warm conveyor belts in the ERA-Interim dataset(1979–2010). Part I: climatology and potential vorticity evolution. J Clim 27(1):3–26. https://doi.org/10.1175/JCLI-D-12-00720.1

Mailier PJ, Stephenson DB, Ferro CAT, Hodges KI (2006) Serial clustering of Extratropical cyclones. Mon Weather Rev 134(8):2224–2240. https://doi.org/10.1175/MWR3160.1

Miao J, Wang T (2020) Decadal variations of the east Asian winter monsoon in recent decades. Atmos Sci Lett 21(4):e960. https://doi.org/10.1002/asl.960

Michaels PJ, Balling RC Jr, Vose RS, Knappenberger PC (1998) Analysis of trends in the variability of daily and monthly historical temperature measurements. Climate Res 10(1):27–33. https://doi.org/10.3354/cr010027

Moberg A, Jones PD, Barriendos M, Bergstrom H, Camuffo D, Cocheo C, Davies TD, Demaree G, Martin-Vide J, Maugeri M, Rodriguez R, Verhoeve T (2000) Day-to-day temperature variability trends in 160-to 275-year-long European instrumental records. J Geophys Res 105(D18):22849–22868. https://doi.org/10.1029/2000JD900300

Nan Y, Sun J, Zhang M, Hong H, Yuan J (2022) Strengthened influence of the east Asian trough on spring extreme precipitation variability over eastern Southwest China after the late 1980s. Atmospheric and Oceanic Science Letters 15(5):100191. https://doi.org/10.1016/j.aosl.2022.100191

Okajima S, Nakamura H, Kaspi Y (2021) Cyclonic and anticyclonic contributions to atmospheric energetics. Sci Rep 11:13202. https://doi.org/10.1038/s41598-021-92548-7

Pickart RS, Moore GWK, Macdonald AM, Renfrew IA, Walsh JE, Kessler WS (2009) Seasonal evolution of Aleutian low pressure systems: implications for the North Pacific subpolar circulation. J Phys Oceanogr 39(6):1317–1339. https://doi.org/10.1175/2008JPO3891.1

Priestley MDK, Catto JL (2022) Future changes in the extratropical storm tracks and cyclone intensity, wind speed, and structure. Weather and Climate Dynamics 3:337–360. https://doi.org/10.5194/wcd-3-337-2022

Ren X, Yang X, Chu C (2010) Seasonal variations of the synoptic-scale transient eddy activity and polar front jet over East Asia. J Clim 23(12):3222–3233. https://doi.org/10.1175/2009JCLI3225.1

Rigby JR, Porporato A (2008) Spring frost risk in a changing climate. Geophys Res Lett 35(12):L12703. https://doi.org/10.1029/2008GL033955

Rohde R, Muller R, Jacobsen R, Perlmutter S, Rosenfeld A, Wurtele J, Curry J, Wickham C, Mosher S (2013) Berkeley earth temperature averaging process. Geoinformatics Geostatistics An Overview 1(2):20–100. https://doi.org/10.4172/2327-4581.1000103

Rosenfeld A (1976) Digital picture processing. Academic press, London

Schär C, Vidale P, Lüthi D, Frei C, Häberli C, Liniger MA, Appenzeller C (2004) The role of increasing temperature variability in European summer heatwaves. Nature 427:332–336. https://doi.org/10.1038/nature02300

Schneider T, Bischoff T, Płotka H (2015) Physics of changes in Synoptic Midlatitude temperature variability. J Clim 28(6):2312–2331. https://doi.org/10.1175/JCLI-D-14-00632.1

Screen JA (2014) Arctic amplification decreases temperature variance in northern mid-to high-latitudes. Nat Clim Change 4:577–582. https://doi.org/10.1038/nclimate2268

Seneviratne SI, Corti T, Davin EL, Hirschi M, Jaeger EB, Lehner I, Orlowsky B, Teuling AJ (2010) Investigating soil moisture–climate interactions in a changing climate: a review. Earth-Sci Rev 99(3–4):125–161. https://doi.org/10.1016/j.earscirev.2010.02.004

Shi L, Kloog I, Zanobetti A, Liu P, Schwartz JD (2015) Impacts of temperature and its variability on mortality in New England. Nat Clim Change 5(11):988–991. https://doi.org/10.1038/nclimate2704

Shin S-H, Moon J-Y (2018) Prediction skill for the east Asian Winter Monsoon based on APCC multi-models. Atmosphere 9(8):300. https://doi.org/10.3390/atmos9080300

Sinclair MR (1997) Objective identification of cyclones and their circulation intensity and climatology. Weather Forecast 12:595–612. https://doi.org/10.1175/1520-0434(1997)012<0595:OIOCAT>2.0.CO;2

Song S, Yeh S, Park J (2019) Change in relationship between the east Asian Winter Monsoon and the east Asian jet Stream during the 1998–99 Regime Shift. J Clim 32(18):6163–6175. https://doi.org/10.1175/JCLI-D-18-0844.1

Sun B, Li C (1997) Relationship between the disturbances of east Asian trough and tropical convective activities in boreal winter. Chin Sci Bull 42:500–503 (in Chinese with English abstract)

Sun C, Kucharski F, Li J, Wang K, Kang I-S, Lian T, Liu T, Ding R, Xie F (2019) Spring Aleutian Low weakening and surface cooling trend in Northwest North America during recent decades. J Geophys Research: Atmos 124(22):12078–12092. https://doi.org/10.1029/2019JD031405

Vanos JK, Kalkstein LS, Sanford TJ (2015) Detecting synoptic warming trends across the US Midwest and implications to human health and heat-related mortality. Int J Climatol 35(1):85–96. https://doi.org/10.1002/joc.3964

Vicedo-Cabrera AM, Forsberg B, Tobias A, Zanobetti A, Schwartz J, Armstrong B, Gasparrini A (2016) Associations of inter-and intraday temperature change with mortality. Am J Epidemiol 183(4):286–293. https://doi.org/10.1093/aje/kwv20526811244

Vitasse Y, Rebetez M (2018) Unprecedented risk of spring frost damage in Switzerland and Germany in 2017. Clim Change 149:233–246. https://doi.org/10.1007/s10584-018-2234-y

Wang X, Zhai P, Wang C (2009) Variations in extratropical cyclone activity in northern East Asia. Adv Atmos Sci 26:471–479. https://doi.org/10.1007/s00376-009-0471-8

Wettstein JJ, Mearns LO (2002) The influence of the North Atlantic–Arctic Oscillation on mean, variance, and extremes of temperature in the northeastern United States and Canada. J Clim 15(24):3586–3600. https://doi.org/10.1175/1520-0442(2002)015<3586:TIOTNA>2.0.CO;2

Wolf K, Schneider A, Breitner S, von Klot S, Meisinger C, Cyrys J, Hymer H, Wichmann H-E, Peters A (2009) Air temperature and the occurrence of myocardial infarction in Augsburg, Germany. Circulation 120(9):735–742. https://doi.org/10.1161/CIRCULATIONAHA.108.815860

Wu FT, Fu C, Qian Y, Gao Y, Wang SY (2017) High-frequency daily temperature variability in China and its relationship to large-scale circulation. Int J Climatol 37(2):570–582. https://doi.org/10.1002/joc.4722

Zanobetti A, O'neill MS, Gronlund CJ, Schwartz JD (2012) Summer temperature variability and long-term survival among elderly people with chronic disease. Proc Natl Acad Sci 109(17):6608–6613. https://doi.org/10.1073/pnas.111307010922493259

Zhang Y, Ding Y, Li Q (2012) A climatology of extratropical cyclones over East Asia during 1958–2001. Acta Meteorol Sin 26:261–277. https://doi.org/10.1007/s13351-012-0301-2

Zohner CM, Mo L, Renner SS, Svenning JC, Vitasse Y, Benito BM, Crowther TW (2020) Late-spring frost risk between 1959 and 2017 decreased in North America but increased in Europe and Asia. Proc Natl Acad Sci 117(22):12192–12200. https://doi.org/10.1073/pnas.1920816117